



HAL
open science

Modal analysis of a bistable deployable module with a refined joint model

M.V.B. Santana, M. Hjiaj, P.Z. Berke

► **To cite this version:**

M.V.B. Santana, M. Hjiaj, P.Z. Berke. Modal analysis of a bistable deployable module with a refined joint model. *Engineering Structures*, 2022, 269, pp.114798. 10.1016/j.engstruct.2022.114798. hal-03780598

HAL Id: hal-03780598

<https://hal.science/hal-03780598>

Submitted on 20 Sep 2022

HAL is a multi-disciplinary open access archive for the deposit and dissemination of scientific research documents, whether they are published or not. The documents may come from teaching and research institutions in France or abroad, or from public or private research centers.

L'archive ouverte pluridisciplinaire **HAL**, est destinée au dépôt et à la diffusion de documents scientifiques de niveau recherche, publiés ou non, émanant des établissements d'enseignement et de recherche français ou étrangers, des laboratoires publics ou privés.

Highlights

Subject: Submission to *Engineering Structures* of the manuscript entitled “Modal analysis of a bistable deployable module with a refined joint model” co-authored by M. V. B. Santana, M. Hjjaj and P.Z. Berke

- Assess of the dynamic behavior of a square bistable deployable scissor structure (BDS) module in the deployed state through modal analysis incorporating the influence of internal stresses (specially relevant when member length imperfections are considered)
- Identification of the main design and topological parameters that have a critical influence on the natural frequencies and vibration modes and quantify their effects
- Influence of the applied material pair for inner and outer scissor like elements, finite joint stiffness and member length imperfections (in a stochastic approach) and topological parameters of the module that a designer would potentially adjust for a modular structure to tame its dynamic behavior.

Modal analysis of a bistable deployable module with a refined joint model

M. V. B. Santana^a, M. Hjjaj^a, P. Z. Berke^b

^a*INSA de Rennes – LGCGM/Structural Engineering Research Group, 20 avenue des Buttes de Coësmes, CS 70839, 35708 Rennes Cedex 7, France*

^b*Building, Architecture & Town Planning (BATir) Department CP 194/2, Université Libre de Bruxelles, Avenue Franklin Roosevelt, 50, 1050 Brussels, Belgium*

Abstract

Bistable deployable scissor structures (BDS) are interesting solutions for temporary civil engineering structures having the requirement of rapid erection and use. The transformation and design of BDS have been studied in various works in the literature using numerical simulations based on a quasi-static loading assumption. In contrast, their dynamic behavior and factors influencing it have not yet been extensively investigated. This contribution presents a computational study in which the natural frequencies and vibration modes of a single square BDS module are evaluated, incorporating the effects of the variation of particular design parameters specific to BDS, i.e. the materials used for inner and outer scissors, finite joint stiffness and manufacturing imperfections on the member lengths (in a stochastic approach) and two geometrical parameters of the module. The most dominant parameters are identified, and their effect is quantified, yielding results of practical interest for design and manufacturing that can be used to reach a target dynamic behavior of BDS.

Key words: bistable deployable structures, structural joints, modal analysis, structural dynamics

Email address: mbentosa@insa-rennes.fr (M. V. B. Santana)

Preprint submitted to Journal of Sound and Vibration

July 7, 2022

1
2
3
4
5
6
7
8
9 **1. Introduction**

10
11
12
13
14
15
16
17
18
19
20
21
22
23
24
25
26
27
28
29
30
31
32
33
34
35
36
37
38
39
40
41
42
43
44
45
46
47
48
49
50
51
52
53
54
55
56
57
58
59
60
61
62
63
64
65

Employing transformable structures can be of great interest for temporary structures in civil engineering because of their ease of deployment and rapidity of entering service. A specific class of transformable structures are bistable deployable scissor structures (BDS) that are practically an assembly of beam and hub elements through revolute joints. They exhibit a click-open (snap-through) behavior due to intended geometric incompatibilities between beam members connected as scissors. These incompatibilities induce internal stresses during transformation that are released in the stable folded and deployed configurations. This bistable nature ideally allows for bearing the self-weight of BDS in the deployed state, requiring only limited further bracing and ensuring rapid serviceability [?].

The transformation behavior of BDS has been recently studied rather extensively [?], leading to recommendations on their design procedure [?] and the proposal of a methodology for their shape and topological optimization [? ?]. Among other findings of interest, BDS were observed to be rather sensitive to manufacturing imperfections, including the hinge axis misalignment and beam lengths variations through nonlinear finite element modeling [?]. The spurious effect of these imperfections was found to be attenuated using structural joints with a finite stiffness. This joint compliance is a result of the incorporation of deformable bushings in the hinge, as shown in [?] where a finite stiffness joint finite element, dedicated to BDS was developed.

A significant part of the efforts gathered in the dedicated literature investigate the transformation behavior and design of BDS based on a quasi-static numerical approach, however studies addressing their dynamic behavior in civil engineering applications are very scarce, to the best knowledge of the authors. Vibrations of deployable structures that are not bistable have been addressed

1
2
3
4
5
6
7
8
9 in the literature for aerospace [? ? ? ? ?] and for civil engineering appli-
10 cations [?], none of these have the SLE (scissor like elements) based topology
11 that generates bistability. Addressing structural failure is of prime importance
12 for BDS and extension of the computational study to this aspect is planned
13 as future work. However, the present contribution focuses rather on the vibra-
14 tional behavior of bistable deployable structures. The dangers of the unwanted
15 transformation in service state have been partially addressed in [? ?].

16
17
18
19
20
21 The specific goals and the main novel contributions here are: (i) to assess
22 the dynamic behavior of a square BDS module in the deployed state through
23 modal analysis incorporating the influence of internal stresses (specially relevant
24 when member length imperfections are considered), (ii) to identify the main
25 design and topological parameters that have a critical influence on the natural
26 frequencies and vibration modes and quantify their effects, particularly focusing
27 on (iii) the applied material pair for inner and outer scissor like elements, finite
28 joint stiffness and member length imperfections (in a stochastic approach) and
29 topological parameters of the module that a designer would potentially adjust
30 for a modular structure to tame its dynamic behavior. This clearly defines a gap
31 of knowledge, and giving a contribution to the understanding of the dynamic
32 behavior of BDS, the identification and quantification of effects influencing it
33 are the main original goals of this work.

34
35
36
37
38
39
40
41
42
43
44 This contribution is organized as follows: Section 2 presents the computa-
45 tional tool, the main ingredients of the numerical model employed for BDS,
46 the considered design parameters and their range. Section 3 is dedicated to
47 the computational results and their analysis. Finally, the main conclusions and
48 future research paths are given in Section 4.

1
2
3
4
5
6
7
8
9 **2. Computational model for dynamic analysis**

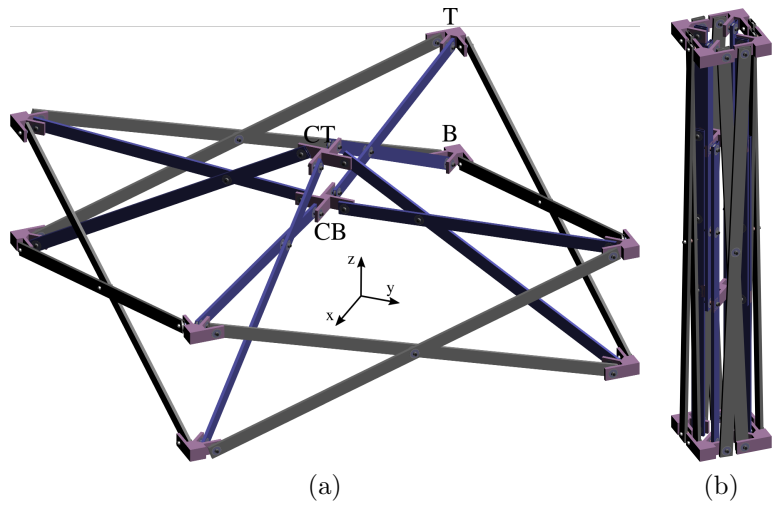
10
11 The computational model set up for the dynamic analysis of a single square
12 bistable module is presented in this section. The necessary details for the under-
13 standing of the behavior of the hinge finite element developed in [?] are recalled
14 first with an original procedure of identifying the joint FE parameters from re-
15 alistic bushing geometries. The derivation of the mechanical response of the
16 joints serves subsequently for feeding the stiffness relationship into the modal
17 analysis. Next, the basic steps of the modal analysis incorporating internal
18 stresses in the deployed state, as a consequence of manufacturing imperfections
19 on the beam length are described. The modal analysis makes use of the stiffness
20 and mass matrices in the deployed state to obtain, via the associated eigenvalue
21 problem, the natural frequencies and vibration modes of the deployable module.
22 Finally, the choice of the selected BDS module parameters and their range for
23 the subsequent dynamic parametric study are given.
24
25
26
27
28
29
30
31
32
33
34

35 *2.1. Computational tool and ingredients*

36
37 The studied square bistable module, shown in Fig. 1 is meant to be part of
38 modular BDS. This module was first proposed by [?] and is composed of beams
39 forming the inner and outer scissors. Its geometry is selected in such a way that
40 the inner SLE are subjected to compressive axial forces and bending moments
41 in both directions of the transformation (opening and closing), which generates
42 the bistable behavior of the system. The force vs displacements transformation
43 curves of this system were studied by many researchers, including more recently
44 in [?], where the effect of the finite stiffness of the joints was considered.
45
46
47
48
49
50

51 In the numerical simulations, each beam half span is discretized into five
52 FE, which is confirmed to be a converged mesh. Each of these 2-noded elements
53 takes into account shear deformations following the Timoshenko beam's theory,
54 i.e. the contribution of the shear stresses in the internal energy and stiffness are
55
56
57
58

1
2
3
4
5
6
7
8
9 considered. The formulation also takes into account large displacements and
10 rotations via the corotational approach [? ?]. Since the joints are modeled
11 as usual finite elements with finite stiffness and inertia, their contributions to
12 the global stiffness and inertia matrices of the system are assembled tradition-
13 ally, with no need to rely on an augmented system of nonlinear equations or
14 penalization. The model in Sec. 3 has a total of 160 elements and 186 nodes,
15 corresponding to 1116 degrees of freedom.
16
17
18
19
20

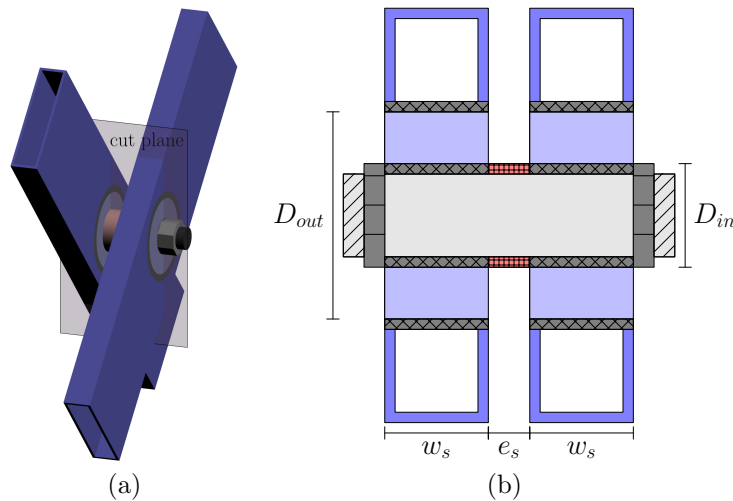


21
22
23
24
25
26
27
28
29
30
31
32
33
34
35
36
37
38 Figure 1: The studied bistable deployable square module in the deployed (a) and in the folded
39 (b) states.
40

41
42 The finite size hubs that serve as connection of more than two beams, sit-
43 uated at the corners and at the intersection of the inner diagonal scissor like
44 elements (SLEs) are also modeled using these beam FE, however a very high
45 stiffness is associated to them to match the usual design assumption that hubs
46 are rigid [? ?].
47
48
49

50
51 Revolute hinges incorporating deformable bushings connect beams to beams
52 and beams to hubs (Fig. 2). These are made of rubber, undergoing small elastic
53 deformations, and are modeled employing the dedicated finite element allow-
54 ing for incorporating a finite stiffness for the radial direction and for rotations
55
56
57
58

1
 2
 3
 4
 5
 6
 7
 8
 9 around axes perpendicular to the hinge axis, referred to as tilting modes (ex-
 10 plained in details later). This finite stiffness models the revolute hinge system in
 11 which two deformable bushings are inserted, its stiffness along these free direc-
 12 tions is a user set parameter that can vary between very large values compared
 13 to the scissor beam stiffness (rigid pinned connection) and low values allowing
 14 for the relative movements of the connected parts that can be useful to com-
 15 pensate for manufacturing imperfections [?]. The axial movement of the hinge
 16 is set strictly to zero, independently of the other stiffness terms to simplify the
 17 model, considering that the axial stiffness of the hinges is expected to not play
 18 a significant role in their structural behavior.
 19
 20
 21
 22
 23
 24
 25
 26



44 Figure 2: Three dimensional view of the embedded deformable hinge in a single scissor showing
 45 the cutting plane (a) in which the details of the proposed technological solution are sketched
 46 with the bushings shown in light blue (b).
 47

48 An important question that was not addressed in [?] is the identification
 49 of the stiffness parameters from actual bushing geometries, which is an original
 50 contribution presented in the following.
 51
 52
 53
 54
 55
 56
 57
 58
 59
 60
 61
 62
 63
 64
 65

2.1.1. Flexible hinge model and parameter identification

The derivation of the radial and tilting stiffness (Fig. 3) of a single cylindrical bushing when linear elastic behavior and small strains are supposed has been established in the literature. The expressions from [?] and [?] serve in this work to obtain the single bushing radial and tilting stiffness, using $E_{\text{bushing}} = 0.8$ GPa [?]. The inner and outer diameters are $D_{\text{in}} = 0.01$ m and $D_{\text{out}} = 0.03$ m and $D_{\text{in}} = 0.02$ m and $D_{\text{out}} = 0.03$ m, with a bushing width of $w_s = 0.01$ m for the soft and hard bushings, respectively. The resulting soft and hard single bushing radial and tilting stiffness values are obtained as $K_r = 3.96 \times 10^7$ N/m and $K_t = 9.40 \times 10^2$ N m/rad and $K_r = 1.87 \times 10^8$ N/m and $K_t = 4.20 \times 10^3$ N m/rad, respectively. The compliant bushings are spaced by a distance $e_s = 0.004$ m (Fig. 2), corresponding to the beams interdistance.

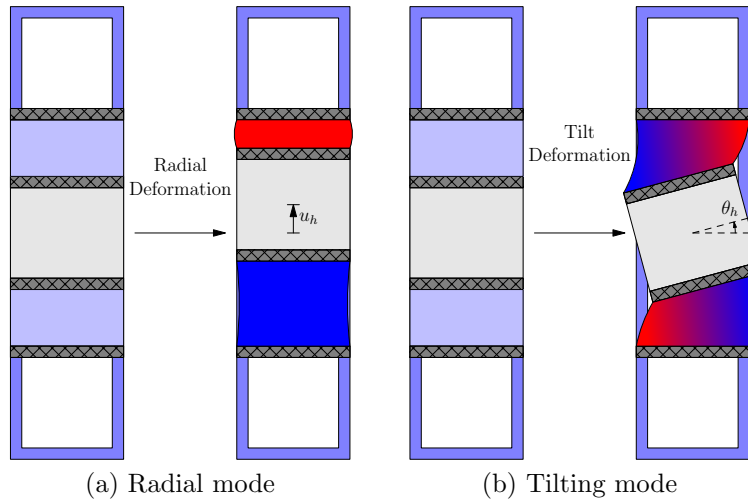


Figure 3: Allowed deformation modes of a single deformable bushing.

Note that in a single beam-beam and beam-hub joint two of these bushings are mounted, as shown in Fig. 2 and the derivation of the stiffness relationships of the associated joint finite element (relating the shearing force to the relative radial displacement u_h in Fig. 4a and the tilting moment to the relative tilting

rotation θ_h in Fig. 4b) is a non-trivial task. The related main equations are given in the following, starting with the relationships describing the kinematics of the two-bushing joint and the force and moment equilibrium allowing to deduce the radial and rotational stiffness for the joint assembly.

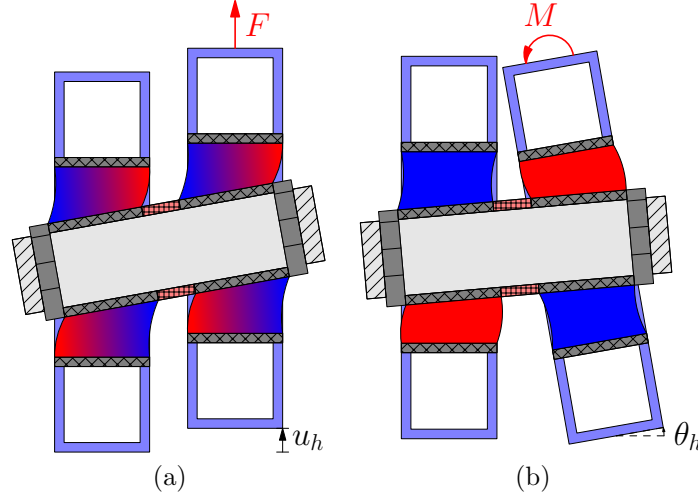


Figure 4: Assumed deformations of the hinge composed of two compliant bushings for shearing load (a) and for a tilting/torsion moment (b).

The pin inserted in the bushings is assumed to move as a rigid body (Fig. 5a) with a displacement u_p and a rotation θ_p , as a result of the deformation of the two compliant bushings. Points B_1 and B_2 are the intersection of the pin axis and the two beam center lines. Their displacements (u_1 and u_2) can be described by the following kinematics:

$$u_1 = u_p - \left(\frac{w_s + e_s}{2} \right) \theta_p \quad (1)$$

$$u_2 = u_p + \left(\frac{w_s + e_s}{2} \right) \theta_p \quad (2)$$

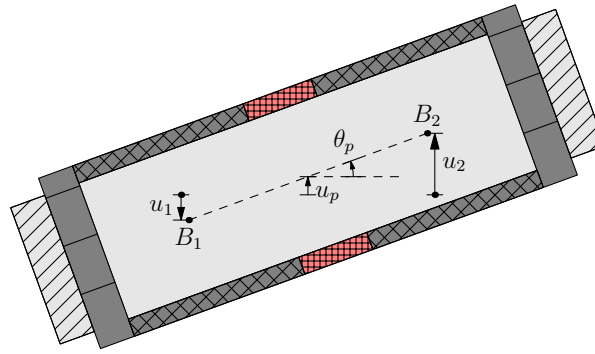
with the beam thickness w_s and spacer size e_s as shown in Fig. 2.

For the sake of simplicity it is assumed that a shearing force induces only relative radial displacement and a tilting moment induces only relative tilting

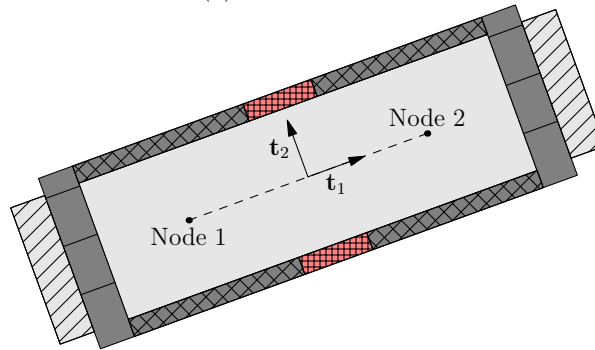
rotation in the finite element formulation, i.e. the coupling of shearing force and relative tilting rotation, θ_h is disregarded in [?].

The assumed deformation of the system for a shearing load is shown in Fig. 4a. The forces acting on the rigid pin are equilibrated by the internal forces due to the radial deformation of the two bushings (Fig. 6a). Considering the relative radial displacement u_h between the two compliant bushings and the single bushing radial stiffness K_r , the following force equilibrium relation can then be derived:

$$K_r u_1 + K_r (u_2 - u_h) = 0 \quad (3)$$



(a) Pin kinematics



(b) Joint FE

Figure 5: Rigid pin in the deformable hinge of a single beam-beam or beam-hub connection and the associated joint FE and its axis.

1
2
3
4
5
6
7
8
9
10
11
12
13
14
15
16
17
18
19
20
21
22
23
24
25
26
27
28
29
30
31
32
33
34
35
36
37
38
39
40
41
42
43
44
45
46
47
48
49
50
51
52
53
54
55
56
57
58
59
60
61
62
63
64
65

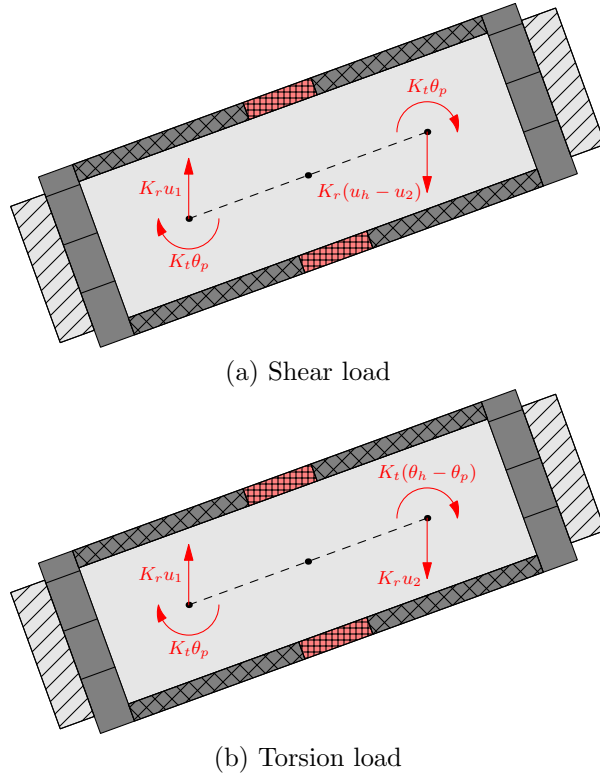


Figure 6: Force and moment free body diagram of the deformable hinge for shear and torsion loads.

Combining Eqs. (1 - 3), the radial displacement of the pin u_p can be obtained as:

$$u_p = \frac{u_h}{2} \quad (4)$$

The moments generated in the pin by the eccentric radial forces and the tilting moments associated to the single bushing tilting stiffness K_t can be related in the following equilibrium equation:

$$2K_t \theta_p + \left(\frac{e_s + w_s}{2} \right) K_r (u_2 - u_h) - \left(\frac{e_s + w_s}{2} \right) K_r u_1 = 0 \quad (5)$$

1
2
3
4
5
6
7
8
9 Combining Eqs. (1 - 2) and Eq. (5), the pin rotation θ_p can be obtained as:

$$\theta_p = \left[\frac{(e_s + w_s) K_r}{4K_t + (e_s + w_s)^2 K_r} \right] u_h \quad (6)$$

10
11
12
13
14
15 Finally, the joint radial stiffness is obtained by taking the equilibrium of
16 forces at the loaded bushing (Fig. 4a):
17
18

$$F = K_r (u_h - u_p) = \frac{K_r}{2} u_h \quad (7)$$

19
20
21
22
23 The assumed deformation of the system for a torsion moment is shown in
24 Fig. 4b. The moments acting on the rigid pin are equilibrated by the internal
25 moments due to the tilt deformation of the two bushings (Fig. 6b). The force
26 equilibrium relation of the rigid pin can be written as:
27
28
29

$$K_r u_1 + K_r u_2 = 0 \quad (8)$$

30
31
32
33
34
35 Combining Eqs. (1 - 2) with Eq. (8), the pin radial displacement u_p can be
36 obtained as:
37
38

$$u_p = 0 \quad (9)$$

39
40
41
42
43 Considering the relative tilt rotation θ_h between the two compliant bushings
44 (Fig. 4b) and the single bushing tilting stiffness K_t , the following moment
45 equilibrium relation can then be derived:
46
47
48

$$K_t \theta_p + K_t (\theta_p - \theta_h) + (e_s + w_s) K_r \left(\frac{e_s + w_s}{2} \right) \theta_p = 0 \quad (10)$$

49
50
51
52
53 Combining Eqs. (1 - 2) with Eq. (10), the rigid pin tilt rotation θ_p can be
54
55
56
57
58

1
2
3
4
5
6
7
8
9 obtained as:

$$\theta_p = \left[\frac{2K_t}{4K_t + (e_s + w_s)^2 K_r} \right] \theta_h \quad (11)$$

10
11
12
13
14
15 Finally, the joint tilt stiffness is obtained by taking the equilibrium of mo-
16
17 ments at the loaded bushing (Fig. 4b):
18

$$M = K_t (\theta_h - \theta_p) = K_t \left[\frac{2K_t + (e_s + w_s)^2 K_r}{4K_t + (e_s + w_s)^2 K_r} \right] \theta_h \quad (12)$$

19
20
21
22
23 From the results above, the joint combined radial stiffness in (Eq. 7) is half of
24
25 the single bushing radial stiffness. The joint combined tilting stiffness (Eq. 12)
26
27 depends on the single bushing radial K_r and tilting K_t stiffness. In the choice of
28
29 dimensions and material parameters of the present work, the term on the single
30
31 bushing radial stiffness K_r in Eq. (12) is very large when compared with the
32
33 term on the single bushing tilting stiffness K_t , and so the joint combined tilting
34
35 stiffness is approximately equal to K_t .

36
37 The details of the joint finite element formulation, including the kinematic
38
39 transformations via the corotational method and the explicit expressions of the
40
41 internal force vector and tangent stiffness matrix, are given in [?]. A flowchart
42
43 of the procedure is shown in Fig. 7. Provided the displacements and rotations
44
45 of the nodes connected to the bushings, the corotational method is used to filter
46
47 the rigid body motion of the joint and capture the portion of the motion that
48
49 causes radial u_h and tilting θ_h movements. A nonlinear constitutive model, that
50
51 uses as parameters the combined bushing stiffness of Eqs. (7) and (12) to feed
52
53 the local stiffness (\bar{k}_0^n and \bar{k}_0^m in [?]), is then applied to obtain the corresponding
54
55 forces and moments in the local system. Finally, these quantities are rotated
56
57 back to the global system, where the equilibrium of the structure is evaluated.
58
59

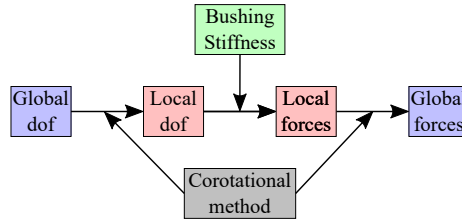


Figure 7: Joint finite element procedure.

2.1.2. Modal analysis accounting for internal stresses

Manufacturing imperfections naturally exist in all engineering structures and BDS were shown to be particularly sensitive to them in [? ?]. Imperfections on the hinge alignment and on the beam length generate spurious deformations and internal stresses in the deployed configuration of BDS, that can be mitigated by the use of deformable joints [?]. These internal stresses are expected to influence the dynamic behavior of BDS as well and should ideally be incorporated in a rigorous investigation when imperfections are considered.

In this work, this is attempted by a two-step approach in which fictitious thermal strains representing unequal beam lengths in the structure are first applied in a static equilibrium problem. The resulting internal stresses are incorporated as geometric stiffness in the subsequent modal analysis that is therefore performed in a deformed equilibrium state in the deployed configuration when member length imperfections are considered. Due to the complexity of the bistable deployable module, specially when considering the flexibility of the joints, analytical models aren't a feasible option and one must then rely on FE models for the modal analysis. The expressions for the beams mass and stiffness matrices and joints stiffness matrices are directly taken from the original works describing their corresponding FE formulations [? ?]. Considering that these references contain exhaustive information, no details are presented

1
2
3
4
5
6
7
8
9 here for the sake of focus and brevity.

10
11 Once the stiffness \mathbf{K}_e and inertia \mathbf{M}_e matrices of each element are assembled
12 into the global stiffness \mathbf{K} and inertia \mathbf{M} matrices of the structure, respectively,
13 the modal analysis of the deployable unit is performed evaluating the eigenval-
14 ues, ω (natural frequencies) and eigenvectors, \mathbf{v} (vibration modes) of the system,
15 via the following symmetric generalized eigenvalue problem,
16
17
18
19
20

$$21 \quad (\mathbf{K}(\mathbf{d}) - \omega^2 \mathbf{M}) \mathbf{v} = \mathbf{0} \quad (13)$$

22
23
24 Here, the stiffness matrix $\mathbf{K}(\mathbf{d}) = \mathbf{K}_m(\mathbf{d}) + \mathbf{K}_g(\mathbf{d})$ depends on the system
25 degrees of freedom \mathbf{d} and so incorporates the effects of internal stresses gener-
26 ated by the gravity load and by initial imperfections. In the present work
27 it's assumed that the damping characteristics of the system are of traditional
28 Aluminum structures (around 1.5% of the critical damping [?]) and therefore
29 having a negligible influence on the natural frequencies of the deployable mod-
30 ule. The routine employed to solve the generalized eigenvalue problem in Eq.
31 (13) is *dsygv* provided in the classical numerical library *Lapack* [?]. The term
32 $\mathbf{K}_m(\mathbf{d})$ corresponds to the material stiffness (depending on the displacements
33 because of the geometrically nonlinear corotational formulation employed here),
34 while $\mathbf{K}_g(\mathbf{d})$ incorporates internal stress induced stiffness, often referred to as
35 geometric stiffness in the literature [? ?]:
36
37
38
39
40
41
42
43
44
45

$$46 \quad \mathbf{K}(\mathbf{d}) = \underbrace{\mathbf{T}^T \bar{\mathbf{K}} \mathbf{T}}_{\mathbf{K}_m} + \underbrace{\frac{\partial \mathbf{T}^T}{\partial \mathbf{d}}}_{\mathbf{K}_g} : \bar{\mathbf{f}} \quad (14)$$

47
48
49
50
51 with $\bar{\mathbf{f}}$ and $\bar{\mathbf{K}} = \partial \bar{\mathbf{f}} / \partial \bar{\mathbf{d}}$ being the internal force vector and (elastic) material
52 stiffness matrix in the corotational system, respectively, and \mathbf{T} is the transfor-
53 mation operator between structural and corotational axes.
54
55
56
57
58
59
60
61
62
63
64
65

1
2
3
4
5
6
7
8
9 When gravity loads and imperfections are considered, the elements internal
10 forces $\bar{\mathbf{f}}$ are first computed via a static nonlinear analysis. The modal analysis
11 of the system is then performed with the tangent stiffness in the deformed
12 configuration and the natural frequencies and vibration modes are computed.
13
14

15 16 17 *2.2. Study parameters*

18
19 The topology, geometrical parameters and dimensions of the studied square
20 bistable module are shown in Fig. 8, where a diagonal cut plane (CT - T - B - CB)
21 is shown. In the subsequent parametric study the thickness of the module ($H =$
22 0.40 m) and the hubs size ($r = 0.05$ m) are kept constant, while the edge length
23 L and top center point height h are varied. The considered boundary condition
24 is setting all degrees of freedom of the bottom central point (CB) to zero, as
25 often applied in transformation simulations [? ?]. Note that establishing more
26 realistic support conditions to mimic the effect of other neighboring modules
27 in a modular structure (e.g. by adding an equivalent stiffness along the square
28 edges) is part of future work.
29
30
31
32
33
34
35

36
37 When the transformation of the module is studied, four horizontal transfor-
38 mation forces are applied on the top nodes of the module in a direction along the
39 square diagonals. In the figures reporting transformation load vs displacement
40 data the magnitude of a single diagonal transformation force F is plotted as a
41 function of the top center point's (CT) vertical displacement w , systematically.
42
43
44

45 The *reference case* is defined as a single square module excluding geometric
46 imperfections, made entirely of Aluminum (specific mass 2700 kg / m³, elastic
47 modulus 70 GPa) with rigid joints, i.e. sufficiently high stiffness to concen-
48 trate the deformation in the scissors only, while ensuring that no numerical
49 ill-conditioning appears. The relative variation in the modal analysis results
50 (e.g. natural frequencies) as a consequence of the variation of different model
51 parameters is measured against this case (which corresponds to the design stud-
52
53
54
55
56
57
58
59
60
61
62
63
64
65

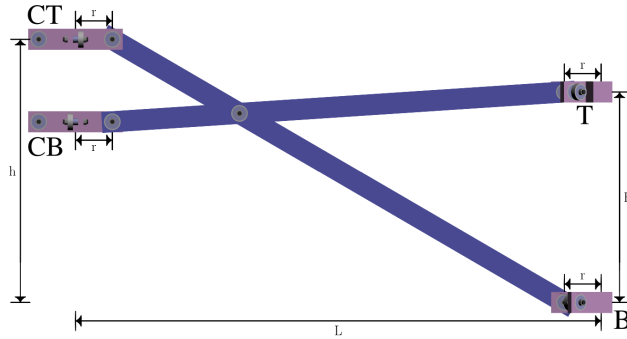


Figure 8: Half-diagonal plane cut of the studied square BDS and corresponding geometric variables.

ied in [?]). All other parameters of the module are given in Tab. 1. The hub size ($r = 0.05$ m) and beams spacing ($s = 0.014$ m) are as proposed in [?] and kept the same in all simulations. The inner and outer scissor beam cross-sections are chosen to be 0.04 m \times 0.01 m with 0.001 m wall thickness. The dimensions chosen for the studied model are the same as the ones presented in references [?] and [?], where it was shown that the module is suitable as a deployable system.

Geometry	
Hub's size (r)	0.05 m
Edge length (L)	1.00 m
Module height (H)	0.40 m
Apex hub height (h)	0.50 m
Joints	
Spacer thickness	0.004 m
Combined tilt stiffness max	3.54×10^3 N m/rad
Combined tilt stiffness min	7.80×10^2 N m/rad
Combined radial stiffness max	1.98×10^7 N/m
Combined radial stiffness min	9.34×10^7 N/m

Table 1: Reference model parameters.

The choice of the materials used for inner and outer scissor beams is a basic degree of freedom in BDS design [?]. In these structures the buckling that

1
2
3
4
5
6
7
8
9 induces the snap-through behavior during transformation is limited to the inner
10 scissors. Increasing the elastic stiffness of these beams by the appropriate choice
11 of the material leads to a higher peak force required for module transformation
12 and a higher structural stiffness in the deployed service state. Choosing a ma-
13 terial with low stiffness for the inner scissor beams can also be a viable strategy
14 when aiming for a reduction of this peak force to allow human force induced
15 transformation. Considering the above, a case in which the inner scissor beams
16 are made of HDPE [?] (specific mass 940 kg / m^3 , elastic modulus 0.8 GPa),
17 while the outer ones are Aluminum will be studied to assess the effect of the
18 material pair choice on the dynamic behavior of the module.
19
20
21
22
23
24
25

26 A given modular structure, with fixed volume, can be constructed with dif-
27 ferent number of modules, by controlling the size of the modules. Reducing the
28 size of a single square module (i.e. the length of the square edge, L) naturally
29 implies shorter scissor beams resulting in the variation of the module stiffness
30 and consequently of its natural frequencies. This effect is considered in this
31 work by varying the square module edge length with respect to the reference
32 case.
33
34
35
36
37
38

39 Another geometrical design parameter incorporated here is the top center
40 point (CT) height at the intersection of the inner diagonal scissors, h , shown
41 in Fig. 8. Increasing this height was shown to result in a higher transformation
42 peak force in [?] with a high sensitivity on this parameter. Changing h is
43 a viable manipulation to tune the peak force of transformation in the design
44 and since it modifies the orientation of the inner scissors it may also have an
45 impact on the module's dynamic behavior, which motivates incorporating it in
46 this study.
47
48
49
50
51
52

53 The cross-section geometry influences the mass and stiffness matrices via its
54 area (A) and moments of inertia (J , I_{22} and I_{33}). In the order to keep the focus
55
56
57
58
59
60
61
62
63
64
65

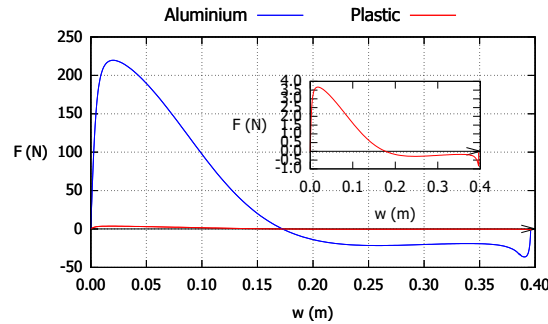
1
2
3
4
5
6
7
8
9 on external geometrical parameters, the influence of the section geometry on the
10 natural frequencies and vibration modes is not considered in the present work.
11 The procedure to incorporate them would be analogous to the one used for the
12 other parameters, computing the natural frequencies and vibration modes via
13 the obtained mass and stiffness matrices.
14
15
16

17
18 Previous work [?] shows that the behavior of deformable hinges and man-
19 ufacturing imperfections [?] have a large influence on the transformation
20 response of BDS. It is naturally expected that the hinge behavior and such im-
21 perfections impact the dynamic structural response as well, which is why they
22 are assessed computationally in a stochastic approach in Sec. 3.2. Note that
23 adjusting the hinge stiffness impacts directly the global structural stiffness, but
24 a very low hinge stiffness may also allow for new vibration modes to appear,
25 resulting in more freedom of deformation of the module. In all the analyses
26 presented in the following a single model parameter is varied while keeping the
27 others at their nominal values given for the reference model. The transforma-
28 tion load vs displacement curves of the module will therefore be reported in this
29 work as well, when relevant.
30
31
32
33
34
35
36
37
38
39

40 **3. Modal analysis of bistable deployable structures**

41
42
43 First the results for the reference pure Aluminum model, i.e. excluding man-
44 ufacturing imperfections and supposed to be built with rigid hinges are presented
45 first. In the present work, all the transformation load vs displacement curves
46 are obtained with a displacements driven algorithm, where the vertical degree
47 of freedom of the top node is controlled. The transformation load vs top central
48 point vertical displacement curve is shown in Fig. 9, exhibiting clearly a bistable
49 nature: the force required to fold the initially deployed structure increases first
50 with increasing displacement, followed by a force decrease leading to a range
51
52
53
54
55
56
57
58
59
60
61
62
63
64
65

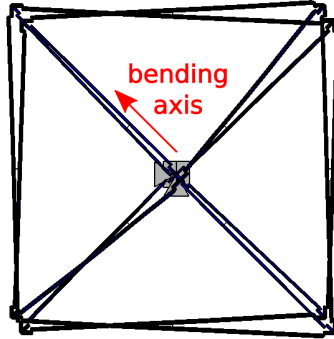
1
2
3
4
5
6
7
8
9 where this force is negative and ending at the compact folded equilibrium con-
10 figuration with a zero external load required.
11
12



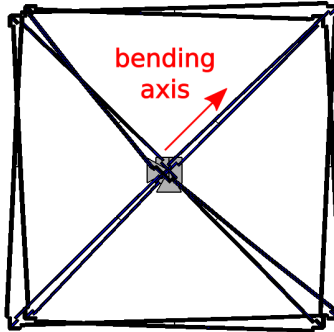
13
14
15
16
17
18
19
20
21
22
23
24 Figure 9: Transformation load vs displacement curves for different material pairs.
25
26

27 The presentation of the modal analysis results is limited to the first three
28 modes in this work, since after careful numerical investigation these have been
29 shown to be the most critical, having the lowest natural frequencies that can
30 be close to the ones of possible excitations encountered in the service state (e.g.
31 wind and/or machinery induced vibrations). For reference, the fourth natural
32 frequency of the pure Aluminum reference case is 3.8 times larger the third nat-
33 ural frequency, being therefore associated to higher energy deformation modes
34 and less likely to be activated by usual loads occurring in civil engineering appli-
35 cations. The mode shapes are shown in different views on Fig. 10. The two first
36 modes with the same natural frequencies are bending modes (bending around
37 the x and y axes), followed by a third torsional mode (around the z axis). This
38 torsional mode is of special interest, since a similar buckling deformation of
39 the inner scissors is observed during the transformation [?]. Hence, exciting
40 this torsional mode by external dynamic loading may lead to unwanted inter-
41 ference with the transformation behavior of the structure. These same modes,
42 i.e. two bending modes with bending axes perpendicular to each other and a
43 torsion mode characterize the modules studied in this work and the focus will
44
45
46
47
48
49
50
51
52
53
54
55
56
57
58
59
60
61
62
63
64
65

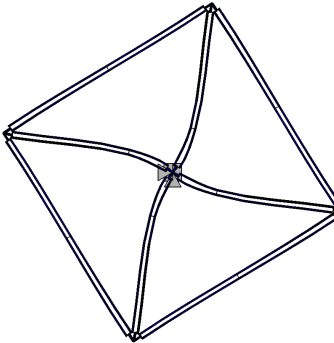
1
2
3
4
5
6
7
8
9 be therefore set on the variation of the natural frequencies of the structure.



22 (a) 1st vibration mode: bending around first diagonal.



35 (b) 2nd vibration mode: bending around second diagonal.



48 (c) 3rd vibration mode: torsion around vertical axis.

49 Figure 10: Top view of the first three vibration modes of the module in the deployed state.

50
51
52
53 The natural frequencies of the pure Aluminum reference case are reported
54 in Tab.2. It is noteworthy that the two first modes have the same natural
55 frequency. This comes as a consequence of the symmetry of the model, as they
56
57
58

are related to the bending of the module with respect to the two symmetry axes in the horizontal plane. The natural frequencies of the first three modes of the reference case are expected to be the highest among all studied cases of the same geometry without imperfections, since this setup corresponds to the stiffest material used for the beams that are linked with a rigid hinge (this is confirmed in Sec. 3.2). The obtained natural frequencies for the studied class of deployable modules falls in the range of usual civil engineering applications ([? ?]).

f [Hz]			
Al	3.18	3.18	5.02
Al-HDPE	0.48	0.48	0.71

Table 2: First three natural frequencies of the structure built from different material pairs.

3.1. Material and geometrical parameters

This section investigates the effect of changing the material to HDPE for the inner scissors that buckle during transformation and the variation of the square module's edge length and the height of the top center point. Fig. 9 shows the dominant impact of the HDPE inner scissors on the transformation response of the module. The peak force magnitude is roughly fifty-fold decreased as a result of the reduction of the elastic modulus of the inner scissors by a factor of 59.7, which clearly illustrates the nonlinear nature of the structural behavior during transformation. The eigenvalues of the module are reported in Tab. 2 and are 6.6 to 7 times lower than the pure Aluminum reference case. A variation of lesser degree in the natural frequencies than in the transformation peak force (both being related to stiffness quantities) can be explained partially by the decrease in the mass of the structure when changing the material pair that accompanies the decrease in the structural stiffness and in part by the difference between the linear modal analysis and the geometrically nonlinear transformation analysis

1
2
3
4
5
6
7
8
9 assumptions.

10 The first two natural frequencies are the same, corresponding to similar
11 bending vibration modes (around perpendicular axes x and y) and the third
12 vibration mode is torsional, as for the pure Aluminum module. The choice of
13 the material pair thus impacts significantly the transformation and vibrational
14 behavior of the module, as expected, and could be used to target a desired
15 range of natural frequencies. In view of the very low transformation forces that
16 make the structure sensitive to self deployment from the folded configuration,
17 the pure Aluminum structure is studied exclusively in the following.

18 The transformation load vs top center point displacement curves as a func-
19 tion of the edge length L and of the top center point height h are plotted in
20 Fig. 11. The influence of the geometric parameters on the transformation of
21 the module has been studied in [?]. The present work focus on the influence
22 of these parameters on the modal analysis of the structure and its link with
23 the transformation peak load. Reducing the edge length leads to shorter inner
24 scissor length and therefore a higher peak force required for their buckling, as
25 it can be observed on Fig. 11a. Halving the edge length results in an increase of
26 200% in the peak load, while a 50% increase in L roughly halves it. When h is
27 decreased, the magnitude of the geometrical incompatibility also reduces, which
28 was shown to have a dominant effect on the transformation behavior in [?].
29 This trend is confirmed in Fig. 11b, i.e. reducing h to half results in a roughly
30 tenfold decrease in the peak load and in a transformation curve of a different
31 nature exhibiting a close to flat plateau in the positive range.

32 Apart from the transformation behavior, the natural frequencies of the mod-
33 ule are also very sensitive to the variation of these geometrical parameters
34 (Tab. 3). The vibration modes remain similar to the reference case and in the
35 same order, independently of the value of L in the considered range. Reducing
36
37
38
39
40
41
42
43
44
45
46
47
48
49
50
51
52
53
54
55
56
57
58
59
60
61
62
63
64
65

1
2
3
4
5
6
7
8
9
10
11
12
13
14
15
16
17
18
19
20
21
22
23
24
25
26
27
28
29
30
31
32
33
34
35
36
37
38
39
40
41
42
43
44
45
46
47
48
49
50
51
52
53
54
55
56
57
58
59
60
61
62
63
64
65

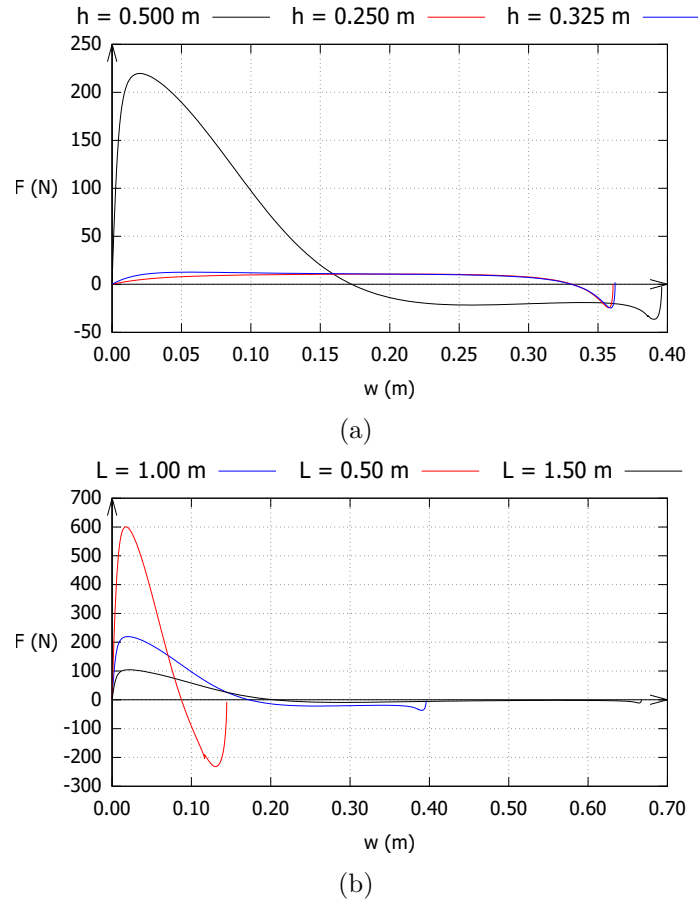


Figure 11: Transformation load vs displacement curves for different geometrical parameters.

the edge length to half results in a 3.4 to 3.8 times increase in the first three natural frequencies, while increasing its value by 1.5 gives natural frequencies that are 41% to 46% of the ones of the reference case; these trends are in line with the one observed for the peak transformation load. Considering the magnitude of these variations, a special attention is thus required when the edge length of such a square bistable module is modified in the design, potentially requiring recomputing not only its transformation but also its dynamic behavior.

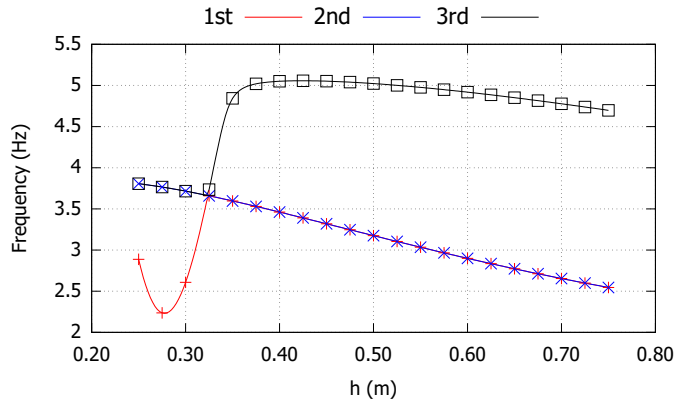
An interesting phenomena occurs when h equals 0.325 m, as shown in Fig. 12a:

h [m]	L [m]	f [Hz]		
0.250	1.00	2.89	3.81	3.81
0.325	1.00	3.66	3.66	3.73
0.500	1.00	3.16	3.16	5.02
0.500	0.50	12.17	12.17	17.35
0.500	1.50	1.29	1.29	2.32

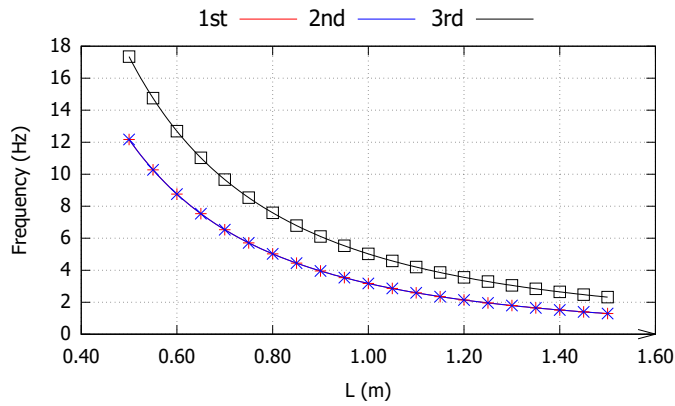
Table 3: First three natural frequencies of the module for different values of the edge length L and of the top center point height h .

at this geometry the three first natural frequencies become the same, which from a practical point of view means that the three first vibration modes are excited simultaneously by a harmonic load at 3.7 Hz. This design should be avoided, because it could induce internal resonance and thereby large magnitude vibrations [? ? ?]. It is noteworthy that for $h < 0.325$ the order of the vibration modes changes, i.e. the torsional vibration mode is first followed by the two bending modes of equal natural frequencies (Tab. 3). Fig. 12a shows the highly nonlinear evolution of the natural frequencies as a function of h exhibiting an abrupt change below 0.37 m and a smooth evolution above. It is emphasized that even though the variation of h , induces a small relative variation in the natural frequencies, it should not be disregarded in a rigorous design approach, since it also impacts the eigenmode order and hence the dynamic structural behavior. The observed small sensitivity of the natural frequencies accompanied by a substantial variation of the transformation peak force can be explained by the different phenomena governing these quantities: structural stiffness in the deployed state and buckling during the transformation, respectively.

The findings above illustrate the complex nonlinear nature of the dynamic behavior of bistable deployable structures and how natural frequencies of such BDS can be adjusted by varying two geometrical parameters of the design, e.g. decreasing the edge length increases the natural frequencies.



(a)



(a)

Figure 12: First three natural frequencies of the module as a function of different geometrical parameters.

3.2. Finite stiffness joints and imperfect member length

The positive influence of having compliant joints in bistable deployable structures in order to decrease the impact of imperfections on the transformation behavior has been established in [?]. In this work finite joint stiffness effects on the *dynamic/vibrational* response of a single square BDS module with the reference geometrical parameter set as nominal values are considered, first in an idealized design geometry lacking manufacturing imperfections, second when incorporating beam length imperfections in the study.

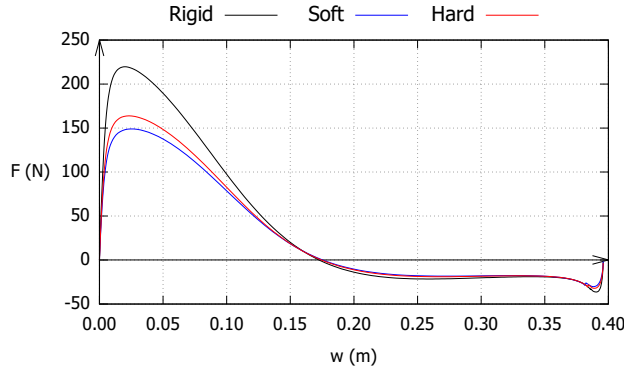


Figure 13: Transformation load vs displacement curves for different hinge stiffness.

For the sake of completeness, the transformation force vs top center point displacement curves for soft and hard joints (as defined in Sec. 2.1.1) are compared to the reference case with rigid joints in Fig.13. It is clearly apparent that incorporating compliance in the hinges is beneficial, since it results in the reduction of the peak transformation load, while the shape of the curve and the part in the negative force range remain practically the same. This implies that additionally to compensating for manufacturing imperfections in the transformation behavior, employing compliant hinges is a practically relevant way in a design for decreasing the force required for transforming BDS without changing the global nature of the curve (as opposed to the top center point height in Fig. 11).

Considering the natural frequencies, a logical decreasing trend is observed in Tab. 4 when the hinge compliance is increased. The natural frequencies of the soft joint case are 74% to 77% of the rigid case (for a peak force decrease of around 68%), which is a moderate variation when compared to the dominant effect of L (Sec. 3.1). It is noteworthy that no vibration mode order change was observed here.

In the following the coupled effect of manufacturing imperfections and joint

Hinge	f [Hz]		
Rigid	3.18	3.18	5.02
Hard	2.52	2.52	4.15
Soft	2.35	2.35	3.90

Table 4: First three natural frequencies of the module for different hinge stiffness.

stiffness on the first three natural frequencies of the BDS module in the deployed state are focused upon. The study is performed in a stochastic framework, considering the length of every beam in the structure as random variable with a uniform distribution. The range of these geometric imperfections in the uniform PDF is chosen to be -0.1% and $+0.1\%$, similar to [?]. They are incorporated as fictitious thermal strains resulting in internal stresses in a preliminary step to the modal decomposition, as explained in Sec. 2. For achieving statistical representativity a total of 50.000 simulations were run for each studied case, i.e. rigid, hard and soft joints.

The resulting probability distribution functions of the first three natural frequencies are plotted in Fig. 14 and indicators of the stochastic data are given in Tab. 5, obtained by fitting a normal PDF to the raw data. As expected, the mean natural frequencies for the three first modes decrease with increasing joint compliance: they are 77%, 80%, 82% and 71%, 75% 77% of the reference case for the hard and soft joint, respectively. Note that the mean values are lower than the one obtained in a deterministic computation without geometrical imperfections (Tab. 4) and the mean natural frequencies of the first and second mode are not the same in the probabilistic approach. It is interesting to point out that the variance in the results systematically increases with the decrease of the joint stiffness, which is an expected result considering that a compliant joint accommodates easier manufacturing imperfections leading to a larger dispersion in the equilibrated configuration used as the basis of the modal analysis. Additionally, the variance in the third, torsional vibration mode appeared to have the largest

relative increase when incorporating finite joint stiffness in the model. It must be emphasized that the initial order of the first two bending modes followed by a third torsional mode was observed systematically in the stochastic study.

Mode	Mean [Hz]	Variance
Rigid		
1	2.99	1.95×10^{-2}
2	3.30	1.10×10^{-2}
3	5.00	4.96×10^{-3}
Hard		
1	2.30	3.03×10^{-2}
2	2.66	1.42×10^{-2}
3	4.12	8.37×10^{-3}
Soft		
1	2.13	3.24×10^{-2}
2	2.49	1.47×10^{-2}
3	3.86	9.59×10^{-3}

Table 5: Statistical data on the first three natural frequencies of the module for different hinge stiffness.

The findings above show that employing compliant hinges in BDS can be recommended as a practical means to (i) decrease the peak transformation force, (ii) manage the spurious effects of geometrical imperfections on the transformation behavior [?], while (iii) maintaining a similar vibrational behavior than when using rigid hinges, only resulting in the decrease of the mean natural frequencies and in an expected increase in the variance in the results when the hinge stiffness is decreased.

4. Conclusions

A computational study was presented in which the natural frequencies and vibration modes of a single square BDS module were evaluated, incorporating the effects of the variation of particular design parameters (material choice, geometric parameters, finite joint stiffness) and manufacturing imperfections. The first three vibration modes were two bending and a third torsional mode in the

1
2
3
4
5
6
7
8
9
10
11
12
13
14
15
16
17
18
19
20
21
22
23
24
25
26
27
28
29
30
31
32
33
34
35
36
37
38
39
40
41
42
43
44
45
46
47
48
49
50
51
52
53
54
55
56
57
58
59
60
61
62
63
64
65

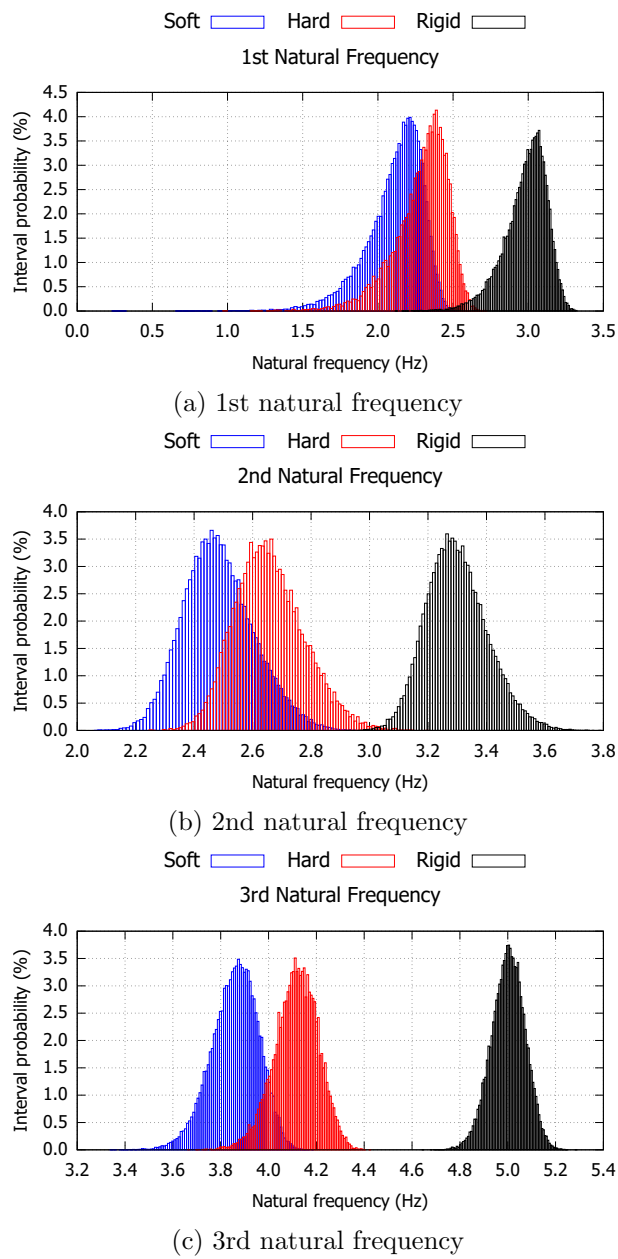


Figure 14: Probability distribution of the natural frequencies of the first three vibration modes when incorporating random member length imperfections for different hinge stiffness.

1
2
3
4
5
6
7
8
9 vast majority of the cases. The torsional mode was observed to be similar to
10 the deformation mode of the structure when transformation takes place and the
11 inner scissors buckle. The first three natural frequencies of the pure Aluminum
12 structure were found between 2 Hz and 5 Hz. The study allowed to identify
13 the dominant influence of the material pair choice for inner and outer scissors
14 and of the edge length of the square BDS module. The top center point height
15 was observed to affect the natural frequencies to a lesser extent, however de-
16 creasing this parameter led to a reversal in the order of the vibration modes, i.e.
17 the torsional mode became the one with the lowest natural frequency. Incor-
18 porating finite joint stiffness led to the decrease of the natural frequencies, as
19 expected. When it was coupled to taking geometric imperfections into account
20 in a probabilistic approach, it resulted in a larger variance in the results, while
21 maintaining a dynamic response similar to the reference case with rigid hinges.
22

23 The presented results illustrate the complex nonlinear nature of the dynamic
24 behavior of bistable deployable structures and show how their natural frequen-
25 cies can be adjusted by making practical design choices. Incorporating com-
26 pliant hinges in the design can be clearly recommended, since (i) it was shown
27 to compensate for manufacturing imperfections in the transformation behavior,
28 (ii) it is a practically relevant way in a design for decreasing the force required
29 for transforming BDS, while (iii) resulting in a moderate decrease in the natural
30 frequencies and keeping a dynamic behavior similar to the one for rigid hinges.
31 Examples of realistic hinges incorporating two bushings for BDS were presented
32 and the procedure to derive the corresponding hinge FE stiffness was explained.
33 Another practical recommendation is to pay a special attention to the edge
34 length variation in iterative BDS design, potentially requiring recomputing not
35 only the transformation but also the dynamic behavior.
36

37 The present work leaves of course space for future improvement. Note that
38
39
40
41
42
43
44
45
46
47
48
49
50
51
52
53
54
55
56
57
58

1
2
3
4
5
6
7
8
9 establishing more realistic support conditions in the modal analysis to mimic
10 the effect of other neighboring modules in a modular structure (e.g. by adding
11 an equivalent stiffness) is part of future work, as well as considering larger,
12 multimodular structures. The present work focuses on a pure numerical ap-
13 proach for obtaining the modal properties of the system (natural frequencies
14 and vibration modes) yielding results of practical interest, that could indeed be
15 verified and coupled to an experimental study in a future work. Addressing the
16 transformation (deployment) behavior of BDS, incorporating friction as energy
17 dissipation mechanism is also part of future work of immediate interest. For this,
18 a full nonlinear dynamic analysis is required and the effects of snap-through and
19 instabilities, present in bistable deployable structures, must be investigated.
20
21
22
23
24
25
26
27
28

29 **Data Availability Statement**

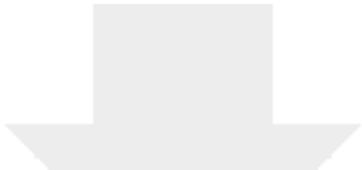
30 The data that support the findings of this study are available from the
31 corresponding author upon reasonable request.
32
33
34
35
36

37 **References**

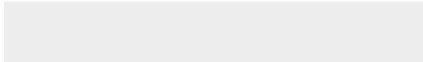
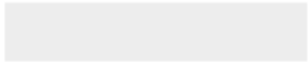
38
39
40
41
42
43
44
45
46
47
48
49
50
51
52
53
54
55
56
57
58
59
60
61
62
63
64
65



Click here to access/download
LaTeX Source File
references.bib



Click here to access/download
Supplementary Material
marked.pdf





Click here to access/download
Supplementary Material
unmarked.pdf

